

Identifying Earth matter effects on supernova neutrinos at a single detector

Amos S. Dagle, Matthias Th. Keil and Georg G. Raelt

Max-Planck-Institut für Physik (Werner-Heisenberg-Institut), Föhringer Ring 6,
80805 München, Germany

Abstract. The neutrino oscillations in Earth matter introduce modulations in the supernova neutrino spectra. These modulations can be exploited to identify the presence of Earth effects on the spectra, which would enable us to put a limit on the value of the neutrino mixing angle θ_{13} and to identify whether the mass hierarchy is normal or inverted. We demonstrate how the Earth effects can be identified at a single detector without prior assumptions about the flavor-dependent source spectra, using the Fourier transform of the "inverse-energy" spectrum of the signal. We explore the factors affecting the efficiency of this method, and find that the energy resolution of the detector is the most crucial one. In particular, whereas water Cherenkov detectors may need a few ten thousand events to identify the Earth effects, a few thousand may be enough at scintillation detectors, which generically have a much better energy resolution. A successful identification of the Earth effects through this method can also provide m^2 to a good accuracy. The relative strength of the detected Earth effects as a function of time provides a test for supernova models.

PACS numbers: 14.60.Pq, 97.60.Bw

1. Introduction

Our knowledge of neutrino masses and mixing parameters has been rapidly improving in the past few years. We know that the neutrino avors e ; and among them selves, and we already have measured the mass squared differences and two of the three mixing angles to a good accuracy [1, 2, 3, 4]. The most important unknowns are the value of the third mixing angle, whether the neutrino mass hierarchy is normal or inverted, and the magnitude of the leptonic CP violation. The neutrino spectra from a core collapse supernova (SN) can shed light on the first two of these unknowns.

Neutrinos produced inside a SN core undergo oscillations on their way out through the mantle and envelope of the star, through the interstellar space, and possibly even through some part of the Earth before arriving at the detector. The spectra of these neutrinos carry information about the two mass squared differences and the e flavor component in the three mass eigenstates. Of course this information comes convoluted with the primary fluxes of the neutrinos produced inside the star, and the extraction of the oscillation parameters depends crucially on our understanding of these primary fluxes.

The uncertainties in the calculations of the primary flux spectra remain large, so only some of the robust features of these spectra can be used with confidence to extract the mixing parameters. Even with this limitation, it has been argued [5, 6] that the observations of the e and ν_e spectra at the detectors on Earth may reveal the type of the neutrino mass hierarchy and imply a range for the third mixing angle. Significant modifications of neutrino spectra can take place if the neutrinos travel through the Earth matter before reaching the detector, and these Earth effects can provide perhaps the most concrete signatures for some of the neutrino mixing scenarios [7, 8, 9].

Any signature of neutrino oscillations depends on the flavor-dependent differences between the primary spectra. Recent studies [10, 11, 12, 13] reveal that these differences are much smaller than had been assumed before. This makes the identification of Earth effects harder than that expected in the previous analyses, and one needs to reevaluate the potential of the detectors from the perspective of these "pessimistic" assumptions about the primary fluxes and spectra.

The comparison of the neutrino signals observed at two detectors would be the most efficient way of detecting the Earth effects. However the detectors need to be sufficiently far apart so that the Earth effects are different for both of them, and sufficiently large to observe a statistically significant signal. Currently Super-Kamiokande is the only large detector that can measure the neutrino energies and can detect more than a few thousands of events from a galactic SN.

Though two detectors, both capable of measuring the neutrino energies, is definitely the most desirable option, it is still possible to detect Earth effects without having to measure the energies of individual neutrinos. Indeed, it has recently been shown that for a galactic SN, the comparison of the number of Cherenkov photons detected at Super-Kamiokande and IceCube as a function of time may be able to identify the Earth effects

[14]. The location of the SN can be anywhere within a specific 70% region of the sky for the effects to be observable.

The motivations to look for a way to identify the Earth effects at a single detector are manifold, the cancellation of systematic uncertainties being the major one. Moreover, in conjunction with the two-detector signature mentioned above, the fraction of the sky for a favorable location of the SN increases to about 85% when Super-Kamiokande is also employed as the "single" detector. For nearly 35% of the sky fraction for the SN location, these two ways of detecting the Earth effects act as complementary tests of each other. The ranges of primary neutrino flux parameters that give an Earth effect signature through these two procedures also differ slightly, since the two-detector method involving IceCube relies on the measurement of integrated luminosity, whereas the one-detector method relies on the analysis of the spectral shape. In this sense, the two methods are complementary to each other.

The naive method of fitting the observed neutrino signal for the primary fluxes and neutrino mixing parameters is inefficient for several reasons. The primary fluxes (their average energies, spectral widths as well as the magnitude of the total fluxes) are time dependent, and only a few rough features can be said to be known with any confidence. One may try to get rid of the time dependence by dividing the signal into several time bins, but this reduces the available statistics. Even within each time bin, one typically has to fit for as many as 5 parameters of the primary spectra, not counting the uncertainties in the neutrino mixing parameters.

However, robust identification of Earth effects can be achieved by observing that the parameters that govern the oscillation frequency of the neutrinos inside the Earth are relatively well measured, and more importantly, completely independent of the primary neutrino spectra. Therefore, the Earth effects can be identified merely by identifying the presence of this oscillation frequency in the observed spectrum. The oscillation frequency does not change with time, thus obviating the need for several time bins. This oscillating component is expected to be a small addition to the otherwise approximately blackbody spectrum that forms the major component of the signal. In order to extract this small oscillation component, we propose a Fourier analysis of the spectrum, which can separate the signals of different frequency from their superposition. We perform a numerical simulation to explore the efficiency of this method at a water Cherenkov detector like Super-Kamiokande, and a large scintillation detector like the one proposed in Ref. [15], which has a much better energy resolution.

Since the Earth effects can be observed only for certain neutrino mixing scenarios, the mere identification of these effects can already tell us whether, for example, the neutrino mass hierarchy is normal. This is a daunting task even at the future long-baseline experiments. In addition, the magnitude of the Earth effects as a function of time gives us important information about the primary neutrino spectra that is extremely useful for understanding the SN dynamics.

This paper is organized as follows. In Sec. 2, we describe the modifications of the primary neutrino spectra by the Earth matter effects. In Sec. 3, we introduce the

Fourier transform for extracting the oscillation frequency of neutrinos inside the Earth, and propose a procedure for identifying the Earth effects without having to make any assumptions about the primary neutrino spectra. In Sec. 4, we explore this method at scintillation and water Cherenkov detectors through a Monte Carlo simulation. Sec. 5 concludes.

2. Neutrino mixing parameters and Earth effects on the ν_e spectrum

Neutrino oscillations are now firmly established by measurements of solar and atmospheric neutrinos and the KamLAND [16] and K2K [17] long-baseline experiments. The weak interaction eigenstates ν_e , ν_μ and ν_τ are non-trivial superpositions of three mass eigenstates ν_1 , ν_2 and ν_3 ,

$$= U_{\nu_i} \nu_i; \quad 2 \text{ fe}; \quad g; i2 \text{ f1;2;3g}; \quad (1)$$

where U is the leptonic mixing matrix. It can be written in the canonical form

$$U = R_{23}(\nu_{23})R_{13}(\nu_{13})R_{12}(\nu_{12}); \quad (2)$$

where $R_{ij}(\nu_{ij})$ corresponds to the rotation in the $i;j$ plane through an angle ν_{ij} . We have neglected the CP violating effects, which are irrelevant for SN neutrinos. From a global 3- flavor analysis of all the available data, one finds the 3 ranges for the mass squared differences m_{ij}^2 , m_i^2 , m_j^2 and mixing angles as summarized in Table 1.

Table 1. Neutrino mixing parameters from a global analysis of all experiments (3 ranges) [1].

Observation	Mixing angle	m^2 [meV 2]
Sun, KamLAND	$\nu_{12} = 27 \{42$	$m_{21}^2 = m_2^2$ $m_1^2 = 55 \{190$
Atmosphere, K2K	$\nu_{23} = 32 \{60$	$j m_{32}^2 j = j m_3^2$ $m_2^2 j = 1400 \{6000$
CHOOZ	$\nu_{13} < 14$	$m_{31}^2 = m_3^2$ m_1^2 m_{32}^2

A SN core is essentially a neutrino blackbody source, but small flavor-dependent differences of the fluxes and spectra remain. Since these differences are very small between ν_e and ν_μ , we represent both these species by ν_x . We denote the fluxes of ν_e and ν_x at Earth that would be observable in the absence of oscillations by F_e^0 and F_x^0 , respectively. For both F_e^0 and F_x^0 , we assume a distribution of the form [12]

$$F(E) = \frac{0}{E_0} \frac{(1 + \beta)^{1+}}{(1 + \beta)} \frac{E}{E_0} \exp(-(\beta + 1) \frac{E}{E_0}); \quad (3)$$

where E_0 is the average energy, a parameter that typically takes on values 2.5–5 depending on the flavor and the phase of neutrino emission, and β the overall flux at the detector. The values of the total flux β and the spectral parameters β and E_0 are different for ν_e and ν_x . We represent these by the appropriate subscripts. Two of the most important robust features of the primary spectra are

- (1) the energy hierarchy of the neutrino species: $hE_{\nu_e} < hE_{\nu_\mu} < hE_{\nu_x}$,

(2) "pinching" of the spectra: $j_{13} > 2$ for all species.

Apart from a heavy water detector like SNO, the neutrino detectors are sensitive mainly to ν_e in the SN energy range. We shall therefore concentrate only on the ν_e spectrum in this paper. In the presence of oscillations a ν_e detector actually observes the flux

$$F_e^D(E) = p_e^D(E) F_e^0(E) + 1 - p_e^D(E) F_x^0(E); \quad (4)$$

where $p_e^D(E)$ is the ν_e survival probability after propagation through the SN mantle and perhaps part of the Earth before reaching the detector. The bulk of the ν_e are observed through the inverse beta decay reaction $\nu_e p \rightarrow n e^+$. The cross section of this reaction is proportional to $E_{\nu_e}^2$, making the spectrum of neutrinos observed at the detector $N(E_{\nu_e}) / F_e^D / E_{\nu_e}^2 F_e^D$.

A significant modification of the survival probability due to the propagation through the Earth appears only for those combinations of neutrino mixing parameters shown in Table 2. The Earth effects depend strongly on two parameters, the sign of m_{32}^2 and the value of j_{13} [5, 7]. The "normal hierarchy" corresponds to $m_1 < m_2 < m_3$, i.e. $m_{32}^2 > 0$, whereas the "inverted hierarchy" corresponds to $m_3 < m_1 < m_2$, i.e. $m_{32}^2 < 0$. Note that the presence or absence of the Earth effects discriminates between values of $\sin^2 j_{13}$ less or greater than 10^{-3} , i.e. j_{13} less or larger than about 1.8° . Thus, the Earth effects are sensitive to values of j_{13} that are much smaller than the current limit.

Table 2. The Earth effects appear for the indicated avors in a SN signal.

13-Mixing	Normal Hierarchy	Inverted Hierarchy
$\sin^2 j_{13} < 10^{-3}$	ν_e and $\bar{\nu}_e$	ν_e and $\bar{\nu}_e$
$\sin^2 j_{13} > 10^{-3}$	ν_e	$\bar{\nu}_e$

Let us consider those scenarios where the mass hierarchy and the value of j_{13} are such that the Earth effects appear for ν_e . In such cases the ν_e survival probability $p_e^D(E)$ is given by

$$p_e^D = \cos^2 j_{12} \sin^2 j_{e2} \sin(2 j_{e2} - 2 j_{12}) \sin^2 12.5 \frac{\overline{m^2} L}{E}^{\frac{1}{2}}; \quad (5)$$

where the energy dependence of all quantities will always be implicit. Here j_{e2} is the mixing angle between ν_e and ν_2 in Earth matter while $\overline{m^2}$ is the mass squared difference between the two anti-neutrino mass eigenstates ν_1 and ν_2 in units of 10^{-5} eV 2 , L is the distance traveled through the Earth in units of 1000 km, and E is the neutrino energy in MeV. We have assumed a constant matter density inside the Earth, which is a good approximation for $L < 9000$ km, i.e. as long as the neutrinos do not pass through the core of the Earth.

The energy dependence of p_e^D introduces modulations in the energy spectrum of ν_e . These modulations may be observed in the form of local peaks and valleys in Fig. 1(a), which shows the spectrum of the event rate, F_e^D , at a detector as a function of the

neutrino energy. Fig. 1 (b) shows the same neutrino signal as a function of the "inverse-energy" parameter, defined as

$$y = 12.5/E : \quad (6)$$

Whereas the distance between the peaks of the modulation increases with energy in the energy spectrum, the peaks in the inverse-energy spectrum are nearly equispaced and hence have a single dominating frequency. This makes it easier to distinguish these modulations from random background fluctuations that have no fixed pattern.

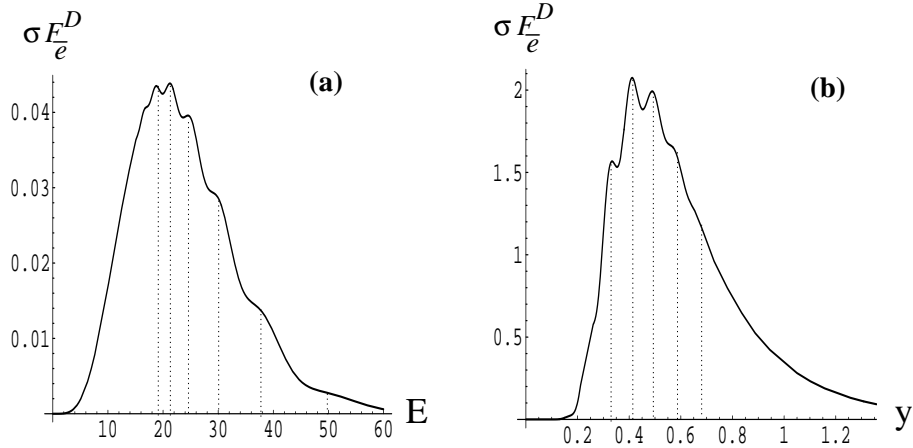


Figure 1. The energy spectrum (a) and the inverse-energy spectrum (b) of F_e^D . The fluxes are normalized such that the area under each curve is unity. For all the examples in this paper, we use the primary neutrino flux parameters $\nu_e = \nu_x = 3.0$, $\hbar E_{\nu_i} = 15 \text{ MeV}$, $\hbar E_{\nu_x} = 18 \text{ MeV}$, $\theta_e = \theta_x = 0.8$, which are realistic for the fluxes during the cooling phase. For the mixing parameters, we use $m^2 = 6$ (in 10^{-5} eV^2) and $\sin^2(2\theta) = 0.9$. The distance travelled through the Earth is $L = 6$ (in 1000 km) unless otherwise specified.

The equidistant peaks in the modulation of the inverse-energy spectrum are a necessary feature of the Earth effects. Indeed, the net ν_e flux at the detector may be written using (4) and (5) in the form

$$F_e^D = \sin^2 \theta_{12} F_x^0 + \cos^2 \theta_{12} F_e^0 + F^0 A \sin^2(\sqrt{m^2} L y) ; \quad (7)$$

where $F^0 = (F_e^0 - F_x^0)$ depends only on the primary neutrino spectra, whereas $A = \sin 2\theta_{e2} \sin(2\theta_{e2} - 2\theta_{12})$ depends only on the mixing parameters and is independent of the primary spectra. The last term in (7) is the Earth oscillation term that contains a frequency $k = \sqrt{m^2} L$ in y , with the coefficient $F^0 A$ being a comparatively slowly varying function of y . The first two terms in (7) are also slowly varying functions of y , and hence contain frequencies in y that are much smaller than k . The dominating frequency k is the one that appears in the modulation of the inverse-energy spectrum in Fig. 1 (b).

The frequency k is completely independent of the primary neutrino spectra, and indeed can be determined to a good accuracy from the knowledge of the solar oscillation parameters, the Earth matter density, and the direction of the SN. If this frequency

component is isolated from the inverse-energy spectrum of ν_e , the Earth effects would be identified. In the next section, we shall show how this can be achieved through the Fourier transform of the inverse-energy spectrum.

3. Identifying the Earth matter effects

3.1. Fourier transform of the inverse-energy spectrum

Taking the Fourier transform of a function is the standard way of extracting components of different frequencies present in the function. The Fourier transform of a function $f(y)$ is

$$g(k) = \int_{-1}^{+1} f(y) e^{iky} dy \quad (8)$$

while the "power spectrum" $G_F(k) = |g(k)|^2$ gives the strength of the frequency k present in $f(y)$.

In Fig. 2 (a), we show the power spectrum $G_F(k)$ of the y -spectrum F_e^D . The peak at $k = 2 m^2 L = 72$ corresponds to the oscillations in Earth matter. The large peak at low values of k , which has the value of unity at $k = 0$, is the dominant contribution due to the first two terms in (7). As may be observed, the Earth effect peak is cleanly isolated from the dominant contribution. The figure also allows us to put a lower bound on the value of k for which the Earth effects will be detectable: if $m^2 L < 20$, the Earth effect peak will be lost in the dominant low frequency peak. Physically speaking, this implies that the neutrinos have to travel a minimum distance through the Earth for the Earth effects to be detectable. So this is not a limitation of this particular method, but a general limitation on the identification of Earth effects.

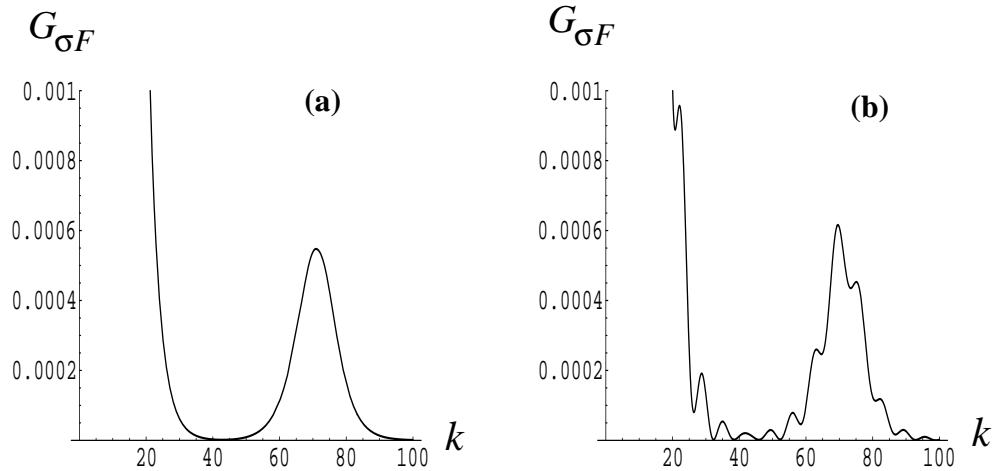


Figure 2. The power spectrum $G_F(k)$ of F_e^D (a) and the same power spectrum with a sharp energy threshold of 10 MeV (b).

The Earth effect peak has a finite width due to the finite y -dependence of the coefficient of the oscillating term $F^0 A$, and of m^2 . The magnitude of the width

is a measure of the y -dependence of these quantities, whereas the area under the peak gives the total contribution of the oscillating Earth effect term.

In Fig. 3(a), we show the envelope of the Earth effect term, $T_F^0 A$, for the typical neutrino spectra parameters during the cooling phase, normalized such that $\int_R F_x^0 dy = 1$. The power spectrum of the Fourier transform $G_T(k)$ of this envelope is shown in Fig. 3(b). Since T is the coefficient of the Earth matter oscillations term $\sin^2(ky)$ and k is nearly constant over all the energy range, the width of the Earth effect peak in Fig. 2(a) is due mainly to the width of $G_T(k)$. We parameterize this width by w , defined as the value of k where $G_T(k)$ is half its maximum value. This would correspond to the halfwidth at halfmaximum of the $k=72$ peak in Fig. 2(a).

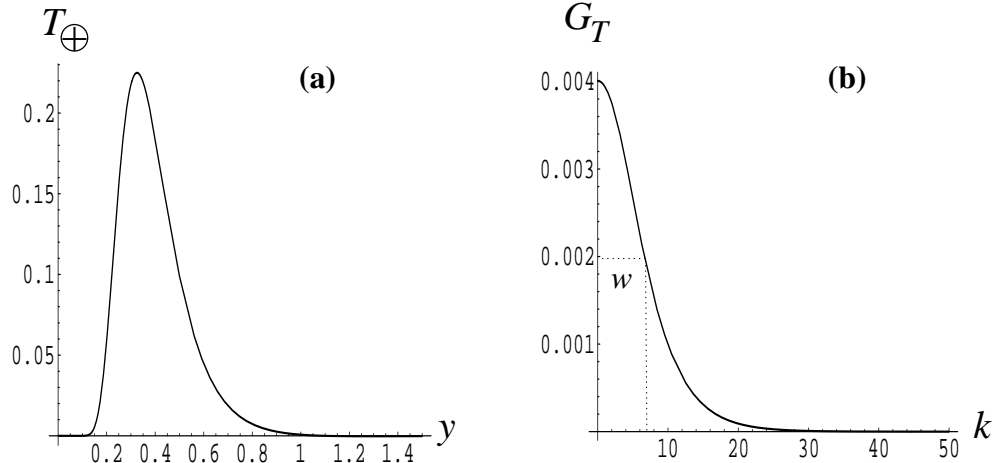


Figure 3. The Earth term $T_F^0 A$ as a function of y , and its power spectrum $G_T(k)$.

In Fig. 3(b), we observe $w \approx 7$. The value of w depends on the primary fluxes, but it is in the range of 3–10 for almost all the allowed parameter range. The exact value of w is not crucial for this analysis, however this estimation is useful in two ways. It allows us to get rid of spurious peaks by applying a selection criterion of a minimum width of the peak, and it also gives us the maximum range of k -values around the mean k for which the Earth effect term contributes.

The neutrino detectors have an energy threshold of about 5–10 MeV, which corresponds to $y = 1.25\{2.5$. Although the number of events below this energy threshold is expected to be very small (See Fig. 1), the presence of a sharp threshold may introduce high frequency components in the y -spectrum. Although the threshold is not sharp in real life, we show an extreme example of the effect of a sharp threshold in Fig. 2(b), taking a threshold of 10 MeV. Since the Fourier transform of a step function is a series of equispaced frequencies, we observe that these high equispaced frequencies are superposed on top of the actual $G_F(k)$. The spacing between these frequencies is much smaller than the width of the Earth effect peak, so the observation of the peak and the area under the peak are not much affected, even in this extreme situation. In reality, the energy

threshold is expected to be much smoother and should not affect the identification of the peak and the measurement of its strength. In all the numerical simulations henceforth, we introduce a sharp energy threshold of 5 MeV in order to take care of the threshold effects.

3.2. The background due to statistical fluctuations

Since the spectrum is observed as a discrete set of neutrinos with individual energies (and hence, individual values), we have to approximate $g(k)$ by the discrete sum

$$g(k) = \frac{1}{N_{\text{events}}} \sum_{y=1}^N e^{iky}; \quad (9)$$

where N is the total number of events. The statistical fluctuations in the spectrum can contribute to frequency components that are comparable to k . This acts as a background for the actual Earth effect peak.

The magnitude of this background can be estimated by assuming that the distribution of ky (modulo 2) is completely random. This is definitely a good approximation for large values of k independent of the details of the distribution of y . In this approximation, the sum in (9) above represents a two dimensional random walk with unit step. This implies that the value of $G_N(k)$ obeys an exponential distribution $P(G) = e^{-G}$, which has a mean $= 1.0$ and variance $= 1.0$ independent of the number of events N . The background due to the statistical fluctuations is thus nearly 1.0 on average, and the "signal" of the peak should rise above this average level in order to be identified.

This is illustrated in Fig 4 (a), where the distance travelled by the neutrinos through the Earth is $L = 0$. Note that the low frequency background is dominant for $k < 40$. In Fig. 4 (b), we show the same neutrino signal, but now with $L = 6$. The Earth effect peak stands out above the background. Though the level of the background is not affected by the number of events, the magnitude of the signal grows proportional to N . Clearly, the Earth effect peak would grow above the background level when the number of events is sufficiently high.

Although the peak identification may be possible "by eye" in many cases, as in Fig 4 (a), the standard particle physics method of resonance identification may be employed for the task. Firstly, we apply a lower k -cut to cut away all $k < k_{\text{cut}}$, where k_{cut} is the value of k where the dominant peak falls to the background level. In Fig 4 (a), for example, $k_{\text{cut}} = 40$. Although we have made a rough estimate of the background above, the actual background may be calculated by averaging the spectrum $G_N(k)$ away from the value k , i.e. in the region where we do not expect the Earth effect peak.

We know from Fig. 2 that the halfwidth at halfmaximum of the peak in k should be $\approx 3\{10$. We then expect that most of the Earth effects contribute to values of k within a range of W around the peak, where W may be taken to be $4w$, for example. We can then choose any interval in k with a range of W , and integrate the power spectrum within this range. Applying the Central Limit Theorem to the background

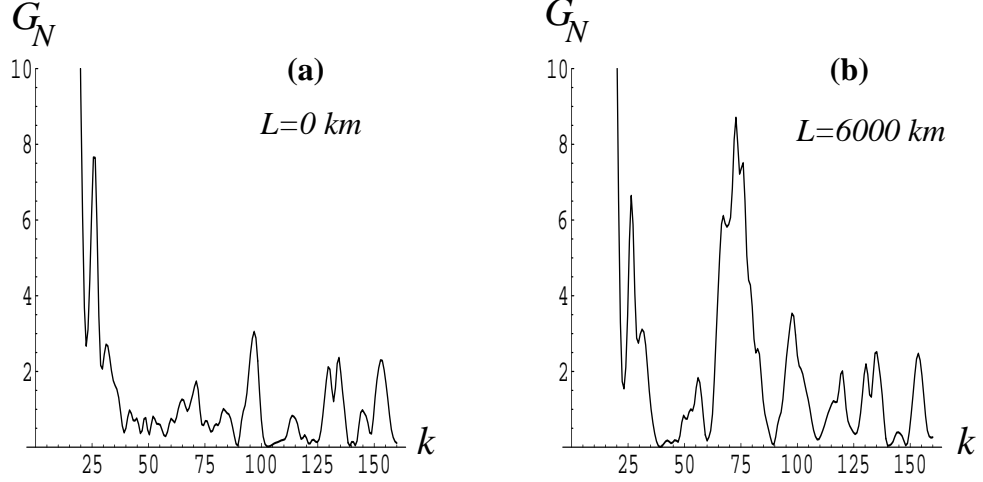


Figure 4. Background due to statistical fluctuations when the Earth effects are absent (a) and the signal peak with the Earth effects (b).

distribution $P(G)$, we can estimate the integral of the background within this interval to be $B = \int_B^W G_N(k) dk$. For $B = 1.0$, $B = 1.0$ and $W = 20$, we get $B = 20 - 4.5$. This implies that $\int_W^R G_N(k) dk > 35$, for example, would correspond to a more than 3 detection of a positive signal. Depending on the actual data, the value of W may be optimized. The procedure of measuring the area under the peak is more efficient than just measuring the peak height since it can weed out the spurious high peaks that do not have the minimum width dictated by $G_T(k)$.

The number of events needed in order to see the signal above the background depends strongly on the primary neutrino spectra, since the coefficient of the Earth effect term depends on F^0 . In Fig. 5(a), we show the Earth effect term $T \sin^2(k y)$ in comparison with the term F_x^0 , normalized such that $\int_R^R F_x^0 = 1$. In Fig. 5(b) we show the normalized term F_x^0 for comparison. The area under this curve is unity. The area A under the curve in Fig. 5(a) may then be taken to be a measure of the net contribution per event of the Earth effect term to the y -spectrum. For the primary spectrum parameters used here, $A = 0.03$ per event.

We show in Fig. 6 the dependence of A on the parameters of the primary spectra. We keep the parameters $x = 3$ and $hE_{ei} = 15 \text{ MeV}$ fixed, and show A as a function of $e^0 = e^0_x$ and hE_{ei} for two typical values of e . During the accretion phase, $e > x$, which is the situation depicted in Fig. 6(a). During the cooling phase, the values for both spectra are very similar, which is depicted in Fig. 6(b). The stars roughly correspond to the parameter values obtained in the SN simulations [13]. It may be observed that for these parameter values, $A = 0.01$ during the accretion phase and $A = 0.03$ during the cooling phase, so that the Earth effects during the accretion phase are expected to be much smaller. The relative magnitude of these effects thus also provides a test for the SN simulations.

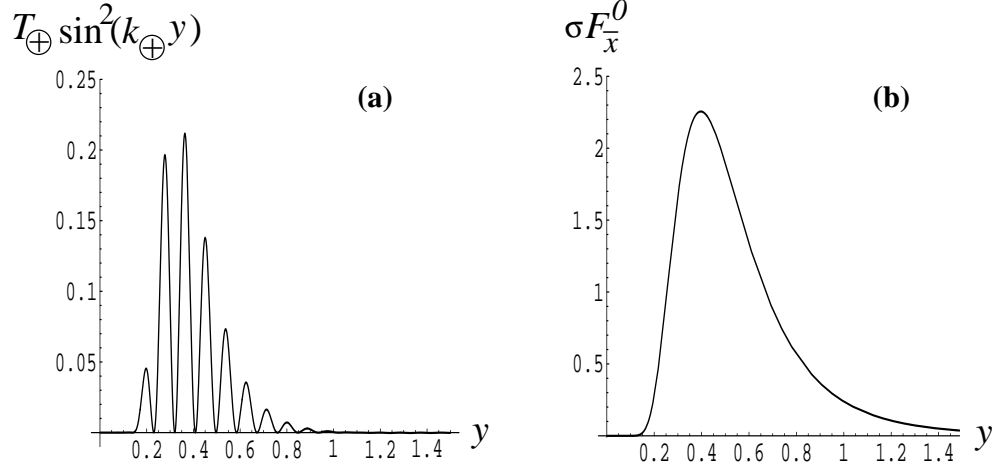


Figure 5. The oscillating Earth effect term, with the cross section of the inverse beta decay factored in (a). It is normalized such that $F_x^0 = 1$. The normalized term F_x^0 is shown in (b) for comparison. Note that the scale in (b) is 10 times the scale in (a).

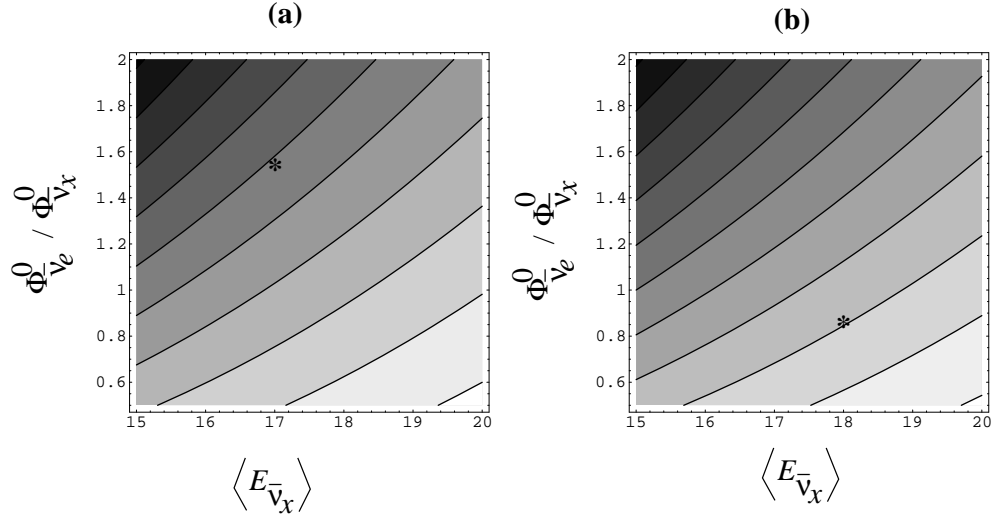


Figure 6. The dependence of A , the area under the curve in Fig. 5(a), on the primary neutrino flux parameters. The contour lines have values starting from 0.05 at the lightest end, with decrements of 0.01 going towards the darker regions. The panel (a) uses the parameters $hE_{\nu_e} = 15$ MeV, $\nu_e = 4$, $\nu_x = 3$, panel (b) uses $hE_{\nu_e} = 15$ MeV, $\nu_e = \nu_x = 3$.

We can estimate the number of events required for a peak identification as follows. In order to get a 3^q identification, we need the "signal" contribution S such that $S > 3\frac{2}{S} + \frac{2}{B}$ where $\frac{2}{S} = S$. With $B = 45$, this corresponds approximately to $S > 20$. In order to reach this strength S with an average contribution of $A = 0.03$ per event for example, we need at least $S = A = 700$ events. This is a very rough, and indeed an optimistic, estimate of the minimum number of events needed in order to detect Earth effects unambiguously. In reality, the energy resolution of the detectors tend to

smear out the oscillations and decrease the magnitude of their strength, thus increasing the required number of events. We shall study the effects of the energy resolution of the detectors in Sec. 4 and get a realistic estimate of the number of events needed to identify the Earth effects. The relative strength of the Earth effects for different primary spectra can still be read off from Fig. 6.

Note that the above procedure can be employed without any prior knowledge of k . Actually, if the value of $\overline{m^2}$ and L is known, we already know the value of k to look for. This helps in getting rid of any background due to spurious peaks. On the other hand, if this peak is identified unambiguously, the value of k can help in improving the accuracy of the measurement of $\overline{m^2}$. We shall study this in the next subsection.

3.3. Determination of $\overline{m^2}$

The current range of the solar mass squared difference $\overline{m^2} = (5.5 \pm 19) \times 10^5 \text{ eV}^2$ is obtained mainly through the combination of the limits from Super-Kamiokande and KamiLAND. Although this range is expected to narrow significantly with the future KamiLAND data, it is worthwhile to note that the Fourier analysis of the SN neutrino spectra can also determine this value to an accuracy of a few percent.

Once the Earth matter peak is identified, the value of k gives the value of $\overline{m^2}$ since the value of L should be well known once the SN direction is established. The error in the measurement of the position of the peak may be roughly estimated by $w=k$. Since we expect $w=3 \pm 10$, and k may be as high as $2 \overline{m^2} / L$ (max) ≈ 400 , even this conservatively estimated error may be only a few percent. As long as $k > 40$, which is the minimum value of k for the Earth effects to be detectable, the error due to determination of the peak position is less than 25%.

The value of $\overline{m^2}$ is related to $\overline{m^2}$ by

$$\overline{m^2} = \overline{m^2} \frac{h}{\sin^2 2\theta} + (\cos 2\theta + 2V_E \overline{m^2})^2 \stackrel{i_1=2}{=} (10)$$

where V is the magnitude of the matter potential inside the Earth. In Fig. 7, we show the y -dependence of $\overline{m^2} = \overline{m^2}$ with various values of solar parameters. Since the y -spectrum is significant only for $y > 0.2$, the deviation of this ratio from unity at $y=0.2$ may be taken as a conservative estimate of the error on $\overline{m^2}$ from the SN spectral analysis. The figure shows that for $y > 0.2$, the values of $\overline{m^2}$ and $\overline{m^2}$ differ by less than 25%, and this difference decreases with increasing $\overline{m^2}$ values. Therefore, it may be safely assumed that effectively, we have $\overline{m^2} = \overline{m^2}$ to within 25%.

Combining the error due to the peak determination and the error due to the difference in $\overline{m^2}$ and $\overline{m^2}$, even conservatively the value of $\overline{m^2}$ would be known to within 35%. KamiLAND may have already pinned this value down to a much better precision, however since no other planned experiment would be able to reach a 35% precision on $\overline{m^2}$ in near future, this could be the first confirmation of the $\overline{m^2}$ value measured at KamiLAND. At high values of $\overline{m^2}$ and L , the error due to the peak width as well as the error due to the $\overline{m^2} - \overline{m^2}$ difference decreases and the accuracy in

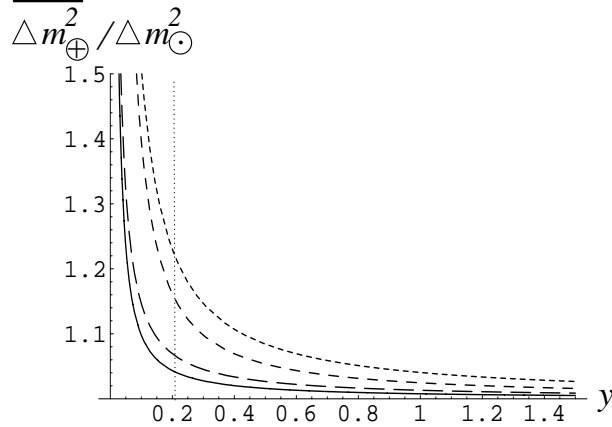


Figure 7. The ratio $\overline{\Delta m_\oplus^2} / \Delta m_\odot^2$ as a function of y for different solar parameters.
 Dotted line: $m^2 = 6 \cdot 10^5 \text{ eV}^2, \sin^2(2_{12}) = 0.7$,
 Short-dashed line: $m^2 = 6 \cdot 10^5 \text{ eV}^2, \sin^2(2_{12}) = 0.9$,
 Long-dashed line: $m^2 = 18 \cdot 10^5 \text{ eV}^2, \sin^2(2_{12}) = 0.7$,
 Solid line: $m^2 = 18 \cdot 10^5 \text{ eV}^2, \sin^2(2_{12}) = 0.9$.

the m^2 measurement may become competitive with KamLAND. For example, with $m^2 = 15 \cdot 10^5 \text{ eV}^2$ and $L = 3000 \text{ km}$, the error in m^2 from the SN spectral analysis would be less than 10%, comparable with the accuracy expected at KamLAND [18].

4. The effect of finite energy resolution

The neutrino signal measured at the detector through the inverse beta decay process $e^-p \rightarrow e^+n$, which is the dominant reaction in both the water Cherenkov as well as the scintillation detector, can be written in the form

$$N_e(E_e) = N_T \int dE_e^0 R(E_e; E_e^0) E(E_e^0) \int dE_e(E_e^0; E) F_e(E) ; \quad (11)$$

where E is the energy of the incoming antineutrino, E_e^0 is the true energy and E_e is the measured energy of the outgoing positron, $(E_e^0; E)$ is the cross section of the inverse beta decay process, E is the efficiency of detection of the positron and $R(E_e; E_e^0)$ is the energy resolution function. The number of target particles is N_T . We neglect the elastic e scattering interactions, which account for less than a few percent of the total number of events, and can even be weeded out through their strongly forward peaked angular distribution.

Since we are interested in the spectral shape observed with a fixed number of total events N , we shall neglect the constant multiplying factors and finally normalize to the number of events using $\int N_e(E_e) dE_e = N$. We take the inverse beta decay process to be completely elastic and isotropic, $(E_e^0; E) / E^2$ everywhere, $E(E_e^0)$ to be uniform over the whole energy range except for a sharp lower threshold of 5 MeV, and $R(E_e; E_e^0)$ to be a Gaussian distribution with mean E_e^0 and the standard deviation D given by the energy resolution of the detector D , where D is SC for a scintillation detector and SK

for a Cherenkov one. The approximations made here retain the essential features of the observed spectra.

The outgoing positrons are detected in the water Cherenkov detectors through the Cherenkov photons that they radiate. In the scintillation detectors, the positrons are detected through photons produced in the scintillation material. Since a larger number of photons can be produced in a scintillation detector, these have typically a much better energy resolution than the water Cherenkov detectors. Indeed, whereas at Super-K amokande we have $_{\text{SK}} 1.5 \text{ MeV} (E=10 \text{ MeV})^{1/2}$ [19], the energy resolution of a scintillation detector may be as good as $_{\text{SC}} 0.22 \text{ MeV} (E=10 \text{ MeV})^{1/2}$ [15], which is more than a factor of 5 better.

Since the identification of Earth effects as described in this paper relies on the detection of the modulations (see Fig. 1), and the finite energy resolution tends to smear them out, it is clear that the energy resolution plays a crucial role in the efficiency of detecting Earth effects. To illustrate this, we show in Fig. 8 the same energy spectrum of the signals as observed at a scintillation and a Cherenkov detector. One can clearly see how the poor energy resolution of the Cherenkov detector smears out the modulations.

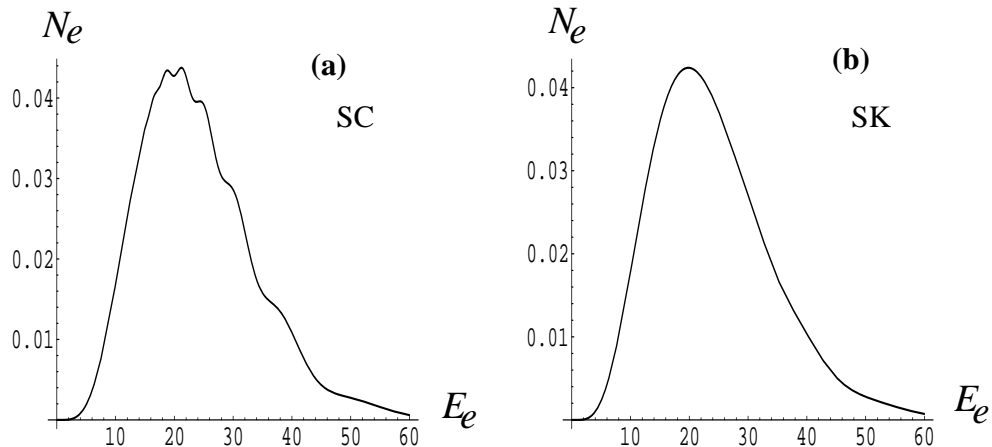


Figure 8. The energy spectrum as observed at a scintillation detector (SC) and a Cherenkov detector (SK). All parameters except the energy resolution are identical.

The difference between Figs. 8(a) and (b) is reflected in the number of events required for the signal to rise above the background at the two detectors. A numerical simulation that generates inverse beta decay events in each of the detectors illustrates the comparative efficiency of the Fourier analyses at these two detectors. In Fig. 9, we show the Fourier transforms of the spectra at these two detectors with 2000 events each. Whereas the peak can be identified even by eye at the scintillation detector, the Fourier power spectrum at the Cherenkov detector is indistinguishable from background.

In Fig 9(a), the area under the peak is around 80. Since the area under the peak grows nearly linearly with the number of events, this indicates that at a scintillation detector, the signal starts becoming visible at around $N = 1000$. At the proposed 50 kiloton scintillation detector LENA [15] for example, one expects about 13,000 events

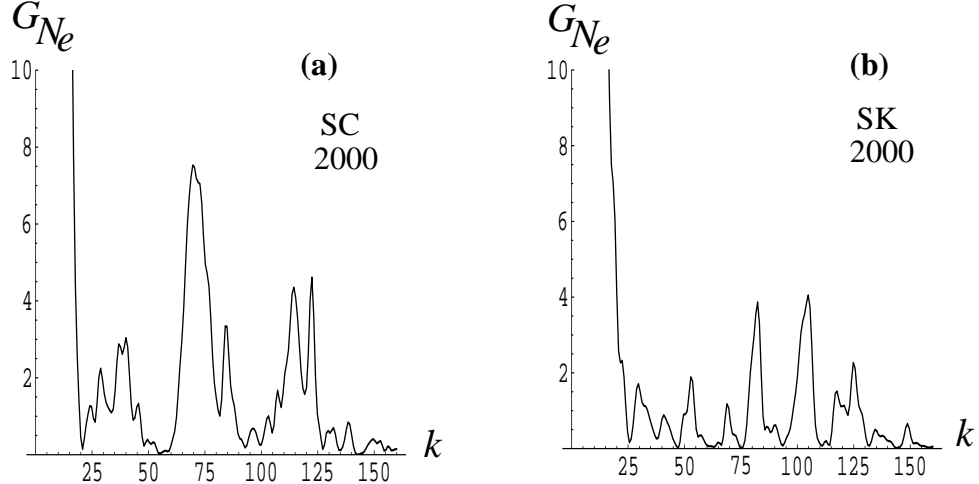


Figure 9. The Fourier transforms of the simulated y-spectra in scintillation and Cherenkov detectors with 2000 events each.

from a SN at 10 kpc. This is an order of magnitude more than the statistics required for identifying the Earth effects. Indeed, a much smaller scintillation detector may be sufficient for this purpose.

At a water Cherenkov detector, the energy resolution is poor compared to a scintillation one. Indeed, the energy resolution is of nearly the same size as the wavelength of the Earth effect modulations for $k \approx 50$. It is therefore much harder to identify the modulations. In Fig. 10(a), we show the Fourier transform of the y-spectra generated at a Cherenkov detector with 100,000 events. We expect that we need more than 60,000 events to be able to identify the peak unambiguously. This indicates that Super-Kamiokande may be too small for detecting the Earth effects by itself in this parameter range. However the proposed Hyper-Kamiokande would have the required size.

If the modulation wavelength is larger than the energy resolution, which is the case for low k , the peak is easier to detect. In addition, if the differences in the primary spectra of e^- and ν_x are larger than those taken in this paper till now, the peak identification can be achieved with a much smaller number of events. In Fig. 10(b), we show the power spectrum with the average energies of the primary spectra differing by 40%, and the value of L decreased to 4000 km. In such a "favorable" range, even a few thousand events would be enough at a water Cherenkov detector, so that Super-Kamiokande has a chance of performing a successful Earth effect detection. However in the light of the latest calculations of SN spectra, such a large energy difference is basically ruled out.

Note that even for a scintillation detector, the energy resolution becomes comparable to the modulation wavelength for large k values, so the number of events required will increase with k . At values of $k > 200$, the modulations get significantly washed out even at a scintillation detector.

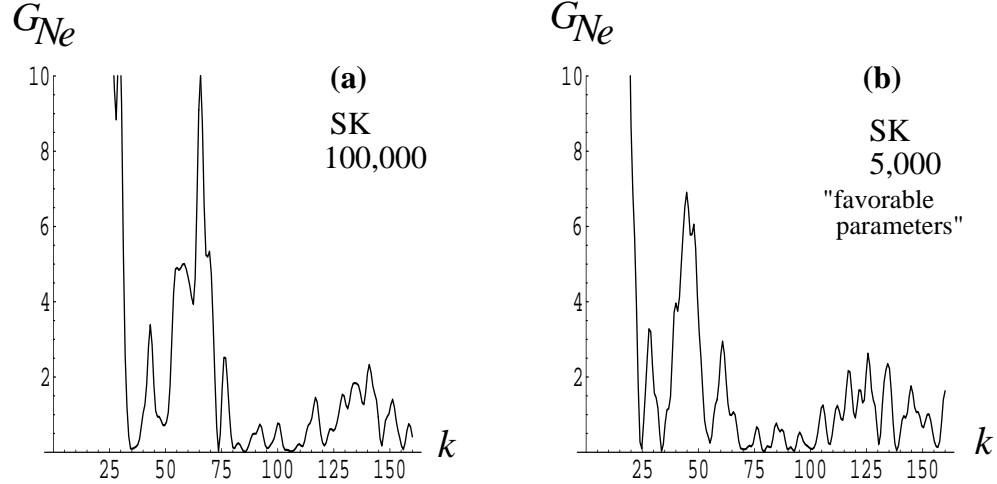


Figure 10. The Fourier transforms of the simulated y-spectra in a Cherenkov detector. (a) uses 100,000 events and the typical neutrino spectral parameters, while (b) uses more extreme "favorable" parameters, $hE_{\nu} = 21$ MeV and $L = 4000$ km. In the latter case, only 5,000 events are enough for the identification of Earth effects.

5. Conclusions

The modulations introduced in the neutrino spectrum by the Earth matter effects provide a way of detecting the presence of these effects without prior assumptions about the flavor-dependent source spectra. We have demonstrated that a Fourier analysis of the inverse-energy spectrum of the ν_e signal may reveal a peak corresponding to the neutrino oscillation frequency in Earth. The position of this peak is insensitive to the primary spectra, and depends only on m^2 and the distance travelled through the Earth. We study the feasibility of the identification of this peak.

The number of events required for an unambiguous identification depends crucially on the energy resolution of the detector. The task is certainly feasible at a large water Cherenkov detector like Hyper-Kamiokande that can detect nearly 10^4 events from a galactic SN. However, scintillation detectors generically have a much better energy resolution than the Cherenkov ones, and typically a scintillation detector can detect the Earth effects with only about 2000 events. This indicates that a scintillation detector large enough to detect a few thousand events from a galactic SN is highly desirable.

The identification of the Earth effects severely restricts the neutrino mixing parameter space, since the effects are present only with certain combinations of the neutrino mass hierarchy and the mixing angle θ_{13} . In particular, if $\sin^2 \theta_{13}$ is measured at a laboratory experiment to be greater than 10^{-3} , then the Earth effects on the ν_e spectrum imply the normal mass hierarchy. However if the Earth effects are not detected, it does not rule out any neutrino mixing parameters, owing to the current uncertainties in the primary fluxes.

A galactic SN is a rare event, expected to occur only a few times per century. However this time scale should be compared with that of those laboratory experiments

which would be sensitive to the mass hierarchy and values of $\sin^2 \theta_{13}$ as low as 10^{-3} . Determination of these two quantities is a difficult challenge even for the experiments that may be running in the next few decades [20, 21, 22]. If a SN is observed within the next decade, the information gained may even be useful in fine-tuning the design parameters of these experiments.

The Fourier analysis described in this paper also yields the value of m^2 to a good accuracy if the matter effects are identified. Though KamLAND should pin down m^2 to within a few percent in the next few years, a galactic SN will provide a completely independent discriminatory test of this value. For large values of m^2 and L , the accuracy in m^2 through the SN spectral analysis becomes comparable with KamLAND.

Models of SNe generically predict time variations in the neutrino flux spectra and hence in the magnitude of Earth effects. The relative strength of the detected Earth effects as a function of time thus provides a test for these models.

In order to reap the benefits of the Earth effects, the detector needs to be shadowed by the Earth from the SN. The probability of such an occurrence is increased by having more than one detector spaced far apart from each other. From the point of view of SN neutrinos, several "small" (a few kiloton) scintillation detectors at different locations are far more useful than a single large one.

Acknowledgments

This work was supported, in part, by the Deutsche Forschungsgemeinschaft under grant No. SFB-375 and by the European Science Foundation (ESF) under the Network Grant No. 86 Neutrino Astrophysics. We thank M. Kachelriess for a careful reading of the manuscript, and R. Tomas for useful discussions.

References

- [1] M. C. Gonzalez-Garcia and Y. Nir, "Developments in neutrino physics," [hep-ph/0202058].
- [2] G. L. Fogli, E. Lisi, A. M. Marrone, D. Montanino, A. Palazzo and A. M. Rotunno, "Solar neutrino oscillation parameters after first KamLAND results," [hep-ph/0212127].
- [3] J. N. Bahcall, M. C. Gonzalez-Garcia and C. Pena-Garay, "Solar neutrinos before and after KamLAND," JHEP 02, 009 (2003) [hep-ph/0212147].
- [4] P. C. de Holanda and A. Y. Smirnov, "Large MSW solution of the solar neutrino problem and first KamLAND results," JCAP 02, 001 (2003) [hep-ph/0212270].
- [5] A. S. Dighe and A. Y. Smirnov, "Identifying the neutrino mass spectrum from the neutrino burst from a supernova," Phys. Rev. D 62, 033007 (2000) [hep-ph/9907423].
- [6] C. Lunardini and A. Y. Smirnov, "Probing the neutrino mass hierarchy and the 13-mixing with supernovae," [hep-ph/0302033].
- [7] A. S. Dighe, "Earth matter effects on the supernova neutrino spectra," [hep-ph/0106325].
- [8] C. Lunardini and A. Y. Smirnov, "Supernova neutrinos: Earth matter effects and neutrino mass spectrum," Nucl. Phys. B 616, 307 (2001) [hep-ph/0106149].
- [9] K. Takahashi and K. Sato, "Earth effects on supernova neutrinos and their implications for neutrino parameters," Phys. Rev. D 66, 033006 (2002) [hep-ph/0110105].
- [10] G. G. Raffelt, "Mu- and tau-neutrino spectra formation in supernovae," Astophys. J. 561, 890 (2001) [astro-ph/0105250].

- [11] R. Buras, H. T. Janka, M. T. Keil, G. G. Raelt and M. Rampp, \Electron-neutrino pair annihilation: A new source for muon and tau neutrinos in supernovae," *Astrophys. J.* 587, 320 (2003) [[astro-ph/0205006](#)].
- [12] M. T. Keil, G. G. Raelt and H. T. Janka, \Monte Carlo study of supernova neutrino spectra formation," *Astrophys. J.*, in press (2003) [[astro-ph/0208035](#)].
- [13] G. G. Raelt, M. Th. Keil, R. Buras, H.-T. Janka and M. Rampp, \Supernova neutrinos: Flavor-dependent fluxes and spectra," *Proc. NOON 03* (10{14 February 2003, Kanazawa, Japan), [[astro-ph/0303226](#)].
- [14] A. S. Dighe, M. T. Keil and G. G. Raelt, \Detecting the neutrino mass hierarchy with a supernova at IceCube," [[hep-ph/0303210](#)].
- [15] L. Oberauer, Talk given at the M P I Colloquium, Munich, April 2003.
- [16] K. Eguchi et al. [KamLAND Collaboration], \First results from KamLAND: Evidence for reactor anti-neutrino disappearance," *Phys. Rev. Lett.* 90, 021802 (2003) [[hep-ex/0212021](#)].
- [17] M. H. Ahn et al. [K2K Collaboration], \Indications of neutrino oscillation in a 250-km long-baseline experiment," *Phys. Rev. Lett.* 90, 041801 (2003) [[hep-ex/0212007](#)].
- [18] A. de Gouvea and C. Pena-Garay, \Solving the solar neutrino puzzle with KamLAND and solar data," *Phys. Rev. D* 64, 113011 (2001) [[hep-ph/0107186](#)].
- [19] M. Nakahata et al. [Super-Kamiokande Collaboration], \Calibration of Super-Kamiokande using an electron linac," *Nucl. Instrum. Meth. A* 421, 113 (1999) [[hep-ex/9807027](#)].
- [20] P. Huber, M. Lindner and W. Winter, \Superbeam sources versus neutrino factories," *Nucl. Phys. B* 645, 3 (2002) [[hep-ph/0204352](#)].
- [21] M. Apollonio et al., \Oscillation physics with a neutrino factory," [[hep-ph/0210192](#)].
- [22] P. Huber, M. Lindner, T. Schwetz and W. Winter, \Reactor neutrino experiments compared to superbeam s," [[hep-ph/0303232](#)].